

7-12-79

INTERIM REPORT
NRC Research and Technical
Assistance Report

Accession No. _____

Contract Program or Project Title: Thermal Fuels Behavior Program

Subject of this Document: "Power-Cooling-Mismatch Test PCM-7 Experiment Predictions"

Type of Document: Experiment Predictions Report

Author(s): R. H. Smith, D. T. Sparks

Date of Document: June 1979

Responsible NRC Individual and NRC Office or Division: R. Van Houten

This document was prepared primarily for preliminary or internal use. It has not received full review and approval. Since there may be substantive changes, this document should not be considered final.

Ray Rose
H. P. Pearson, Supervisor
Information Processing
EG&G Idaho, Inc.

Prepared for
U.S. Nuclear Regulatory Commission
Washington, D.C. 20555

NRC File #A6041

INTERIM R.

NRC Research and Technical
Assistance Report

510 031
28
7908010364

TFBP-TR-321
for U.S. Nuclear Regulatory Commission

**POWER-COOLING-MISMATCH
TEST PCM-7
EXPERIMENT PREDICTIONS**

R. H. Smith D. T. Sparks

June 1979



EG&G Idaho, Inc.



IDAHO NATIONAL ENGINEERING LABORATORY

DEPARTMENT OF ENERGY

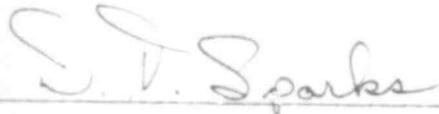
IDAHO OPERATIONS OFFICE UNDER CONTRACT EY-76-C-07-1570

510 032

POWER-COOLING-MISMATCH
TEST PCM-7
EXPERIMENT PREDICTIONS

R. H. Smith
D. T. Sparks

Approved:



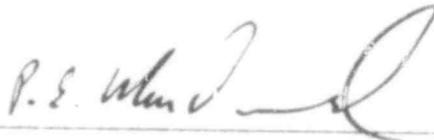
D. T. Sparks, Project Leader PCM Test Series



A. S. Mehner, Supervisor
PCM and RIA Tests Section



R. K. McCardell, Manager
Experiment Specification and Analysis Branch



P. E. MacDonald, Manager
Light Water Reactor Fuel Research Division

EG&G IDAHO, INC.

INTERIM REPORT

Accession No. _____

Report No. TFBP-TR-321**Contract Program or Project Title:**

Thermal Fuels Behavior Program

Subject of this Document:

Experiment Predictions for Test PCM-7

Type of Document:

Experiment Predictions Report

Author(s): R. H. Smith and D. T. Sparks**Date of Document:**

June 1979

Responsible NRC Individual and NRC Office or Division:

R. Van Houten

This document was prepared primarily for preliminary or internal use. It has not received full review and approval. Since there may be substantive changes, this document should not be considered final.

EG&G Idaho, Inc.
Idaho Falls, Idaho 83401

Prepared for the
U.S. Nuclear Regulatory Commission
and the U.S. Department of Energy
Idaho Operations Office
Under contract No. DE-AC07-76ID00-1570
NRC FIN No.

INTERIM REPORT

510 074

The FRAP-T4 model utilized for the PCM-7 test predictions contained in this report have been reviewed and approved by the EG&G Pretest Prediction Consistency Committee.

Michael P Bohm

Fuel Behavior Code Development Representative

W. R. Coleman

Code Assessment Representative

Dave Nebwisse

LOFT Program Representative

Harold Hest

Semiscale Program Representative

CONTENTS

| | |
|--|----|
| SUMMARY | 1 |
| 1. INTRODUCTION. | 4 |
| 2. DESIGN AND SCOPING ANALYSIS | 7 |
| 2.1 Neutronics Calculations. | 7 |
| 2.2 Thermal-Hydraulic Calculations | 10 |
| 2.3 Rod Bowing Calculations. | 12 |
| 2.4 Fuel Rod Behavior Scoping Analysis | 14 |
| 3. EXPERIMENT PREDICTIONS. | 23 |
| 3.1 On-Set of Film Boiling | 23 |
| 3.2 Fuel Rod Behavior. | 24 |
| 4. DISCUSSION. | 32 |
| 5. REFERENCES. | 33 |

FIGURES

| | |
|--|----|
| 1. Schematic of Test PCM-7 nine-rod cluster, showing the locations of the fuel rod instrumentation with respect to the bottom of the fuel stack | 5 |
| 2. Average circumferential power and azimuthal surface heat flux factors per 30° segment of fuel rod based on RAFFLE and TOODEE calculations, respectively, for the 9-rod test assembly | 11 |
| 3. Model of the 9-rod test assembly showing coolant flow sub-channels and corresponding fuel rod segments, used in the COBRA-IV calculations. | 13 |
| 4. Calculated fuel rod displacement due to bowing caused by temperature gradient across the rod from neutron self shielding. | 15 |
| 5. Test PCM-5 assembly showing fuel rod diameters, lattice spacing and shape of flow shroud | 16 |
| 6. Geometry used to simulate single channel analysis of corner, side and center rods | 17 |
| 7. PCM-7 rod cluster peak cladding temperatures after approximately 10 and 20 seconds of film boiling at an inlet coolant temperature of 605 K and a power of 57.1 kW/m. All values inside of rod sketch perimeter are 10 s values outside are 20 s values. | 20 |
| 8. Peak cladding surface temperature as a function of time for corner, side, and center rods of a PCM nine-rod cluster. Inlet temperature 605 K, averaged peak rod power 57.1 kW/m | 22 |
| 9. Axial temperature profile for the cladding surface and fuel centerline calculated by FRAP-T for an average corner rod at a peak power of 57.1 kW/m, coolant inlet temperature of 605 K, and mass flux of 1736 and 1163 kg/s·m ² (3% and 35% below calculated initiation of film boiling) | 25 |
| 10. Peak cladding surface temperature as a function of coolant mass flux percent where 100% represents the point of initial film boiling, PCM-7 corner rod | 26 |
| 11. Ni ³ -ductility temperature as a function of exposure time and temperature from Reference 12. Dashed lines are extrapolations | 27 |
| 12. FRAP-T calculated axial temperature profile for the cladding surface and fuel centerline of a side rod at the 35% flow reduction level (1163 kg/s·m ²). Test rod power of 57.1 kW/m and inlet temperature of 605 K | 30 |

| | | |
|-----|---|----|
| 13. | FRAP-7 calculated temperature profile for the cladding surface and fuel centerline of the center rod at the 35% flow reduction level ($1163 \text{ kg/s}\cdot\text{m}^2$). Test rod power of 57 kW/m and inlet temperature of 605 K | 31 |
|-----|---|----|

TABLES

| | | |
|------|---|----|
| I. | Summary of Calculated Rod Powers for the 9-rod Test Assembly | 9 |
| II. | Film Boiling Flow Rates Calculated by COBRA. | 19 |
| III. | Fuel Rod Response as a Function of Coolant Mass Flux Reduction for the Corner Rods of Test PCM-7. | 28 |
| A-I | Input Parameters, Correlations and Modeling Options Used in the COBRA-IV Calculations. | 36 |
| B-I | Input Parameters, Correlations and Modeling Options Used in the FRAP-T4 Calculations | 40 |

510 038

SUMMARY

The Power-Cooling-Mismatch (PCM) test series is being conducted to better define the response of unirradiated, pressurized water reactor (PWR) type fuel rods under high temperature film boiling conditions. To date, several single-rod tests and one nine-rod cluster test (PCM-5) have been conducted. The objectives of Test PCM-7 are to:

- (1) Evaluate the behavior of a central fuel rod in high temperature film boiling surrounded by other rods also in film boiling
- (2) Determine the integral cluster behavior of a small cluster in high temperature, film boiling operation
- (3) Provide replication of Test PCM-5 results by evaluating the potential for departure from nucleate boiling (DNB) and rod failure propagation
- (4) Provide a direct comparison of fuel rod behavior in a small cluster geometry with previously obtained, single-rod PCM data
- (5) Evaluate the rewet characteristics of the PCM-7 cluster.

The nine fuel rods to be used in the PCM-7 experiment are similar in design to unirradiated 15x15 PWR rods, though they are shorter (0.91 m fuel stack), to accommodate placement in the Power Burst Facility (PBF) test space, and the enrichments are varied to meet power level and power distribution requirements. The test rods are backfilled with helium to cold internal pressures of 2.58 MPa. The nine rods are spaced in a 15X15 PWR lattice by a series of grid spacers, and are surrounded by a nearly square, zircaloy-4 flow shroud. The center fuel rod, one corner rod, and one side rod are instrumented to measure rod internal pressure, fuel centerline

310 039

temperature, cladding surface temperature (in four locations), and cladding axial elongation. Four rods are instrumented for cladding surface temperature only (in two locations), and two are equipped with cladding elongation transducers only. The test train is instrumented to measure thermal neutron flux, coolant pressure, flow rate, coolant temperature, and coolant temperature increase in the test space. These instruments will be used to establish coolant conditions and to calorimetrically determine the cluster power.

Analyses were conducted to predict the test rod behavior and thermal-hydraulic conditions during Test PCM-7. Neutronics calculations performed prior to Test PCM-5, indicated that enrichments of 93, 35 and 20% for the center, side, and corner rods, respectively, would result in a relatively flat rod-to-rod power profile, although the power would be highly skewed toward the outside of the peripheral fuel rods due to neutron self shielding. Measurements of the assembled PCM-5 flow shroud and PCM-5 posttest analysis indicated that asymmetrical positioning of the cluster within the shroud could affect the performance of the assembly. Calculations were performed to scope the thermal-hydraulic conditions at film boiling occurrence using the calculated power skewing and results from Test PCM-5.

The COBRA-IV¹ computer code was used to predict the thermal-hydraulic conditions at the onset of film boiling using both the measured cluster dimensions from Test PCM-5 and nominal shroud dimensions. In both cases, the corner rods were predicted to enter film boiling first, followed by the side rods and finally, the center fuel rod. At a peak rod power of 57.1 kW/m (weighted average peak power per rod), inlet temperature of 605 K, and system pressure of 15.2 MPa, predictions using nominal shroud dimensions (symmetrical cluster positioning) resulted in an expected shroud mass flux at DNB occurrence of 1790 and 1495 kg/s·m² for the corner and side rods, respectively. The measured asymmetry from Test PCM-5 resulted in calculated mass fluxes of; (a) 1880 and 1465 kg/s·m² for the corner rod flow areas (minimum and maximum, respectively), and (b) 1565 and 1385 kg/s·m² for the side rod flow areas (minimum and

maximum, respectively). For all cases evaluated, the predicted mass flux at DNB occurrence on the center rod was $1265 \text{ kg/s}\cdot\text{m}^2$.

Cladding temperatures in the β -phase ($T > 1245 \text{ K}$) zircaloy temperature range were predicted in all rods attaining film boiling conditions. Cladding melting was not predicted. A small amount of fuel melting at the peak temperature locations was calculated. Bowing of the peripheral rods is expected as a result of power skewing, but its effect on the assembly thermal-hydraulics was not quantified. Embrittlement failure of the corner rod is predicted within 10 minutes of film boiling initiation on the center fuel rod.

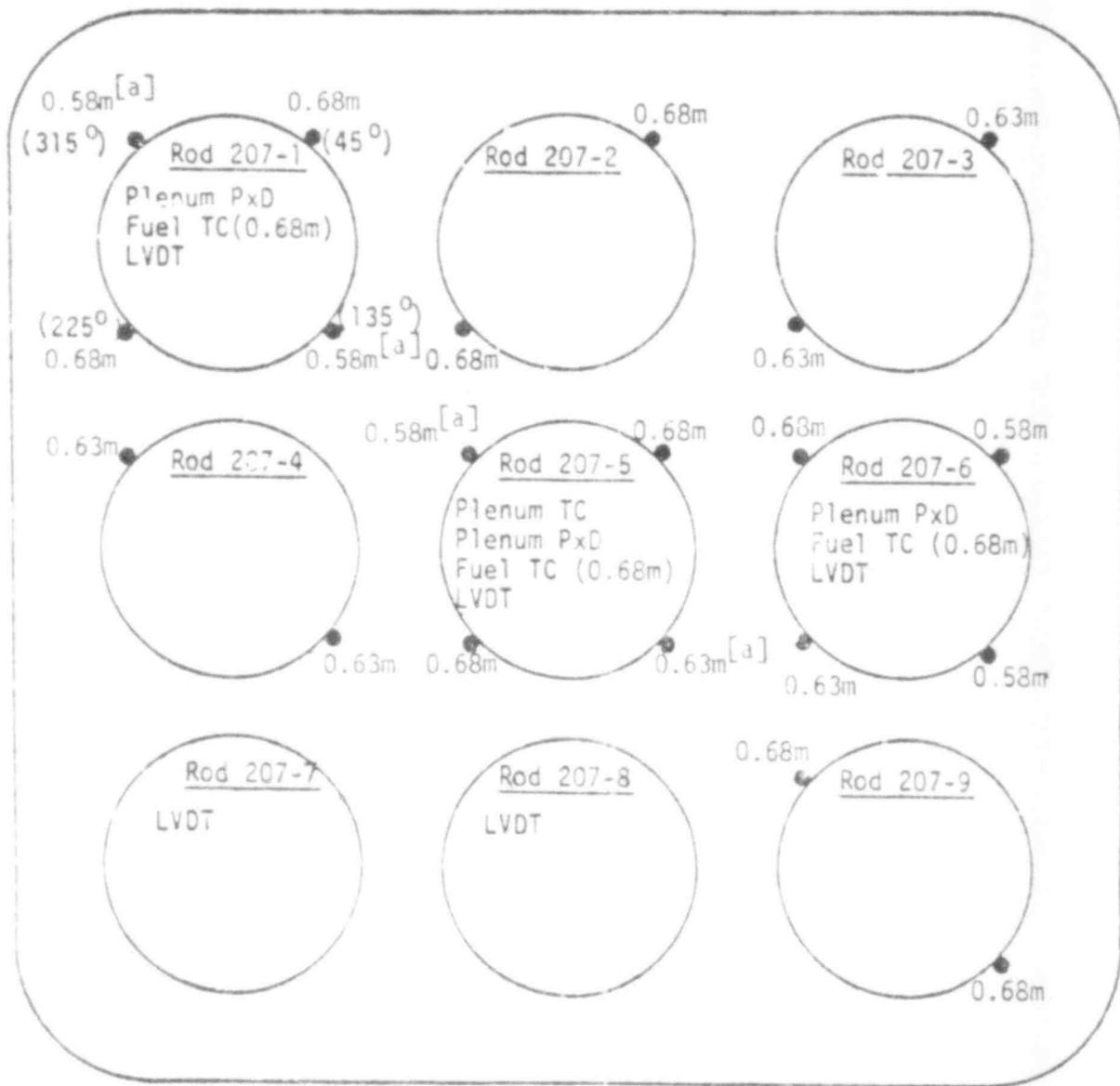
1. INTRODUCTION

The Power-Cooling-Mismatch (PCM) Test PCM-7, discussed in this report, consists of a nine-rod cluster of pressurized water reactor (PWR) type fuel rods (Figure 1) situated in a 3X3 array, with 15X15 PWR lattice spacing between fuel rods. The test will be performed in the Power Burst Facility (PBF).

The general objective of the Power-Cooling-Mismatch (PCM) test series is to provide a base of experimental data for the development and assessment of analytical models and computer codes, used to predict the behavior of light water reactor fuel rods during periods of power and coolant imbalance. In line with the individual test requirements, as defined in the PCM Experiment Requirements Document², Test PCM-7 is to be the second of two experiments designed to study the behavior of fuel rods in a cluster geometry. The objectives of the PCM-7 test are to:

- (1) Evaluate the behavior of a central fuel rod in high temperature film boiling surrounded by other rods also in film boiling
- (2) Determine the integral cluster behavior of a small cluster in high temperature film boiling operation
- (3) Provide replication of Test PCM-5 results by evaluating the potential for departure from nucleate boiling (DNB) and rod failure propagation
- (4) Provide a direct comparison of fuel rod behavior in a small cluster geometry with previously obtained, single-rod PCM data
- (5) Evaluate the rewet characteristics of the PCM-7 cluster.

510 042



[a] Indicates location of the small diameter (0.71 mm) thermocouples

Fig. 1 Schematic of Test PCM-7 nine-rod cluster, showing the locations of the fuel rod instrumentation with respect to the bottom of the fuel stack.

516 043

The test is to be performed under conditions similar to those of Test PCM-5 and previous single-rod PCM tests to provide a direct comparison with the earlier test results.

This report presents the experiment design and the fuel rod behavior experiment predictions analyses. The fuel rods, test hardware, instrumentation, and test conduct are described in the Experiment Operating Specifications³. The analytical procedures, analyses, and computer codes used to determine the experiment design are discussed in Section 2. The fuel rod behavior experiment predictions are presented in Section 3. Discussion of the analytical results are presented in Section 4.

2. DESIGN AND SCOPING ANALYSIS

The Test PCM-7 objective is to study the response of PWR type fuel rods subjected to high temperature film boiling operation in a small cluster geometry. To attain this objective, extensive calculations to evaluate the test design and conduct were performed. Some of the analysis were conducted for Test PCM-5 and, due to the similarities between Tests PCM-5 and PCM-7, were not repeated. Other calculations were conducted on the basis of posttest results obtained from Test PCM-5 to help evaluate the complex interdependence of the local thermal-hydraulic conditions within the cluster. The computer code calculations and the application of the results are summarized in this section.

2.1 Neutronics Calculations

Neutronics calculations⁴ were conducted prior to Test PCM-5 to determine the fuel enrichments required to provide a relatively flat rod-to-rod power generation profile in the nine rod cluster experiments. Due to symmetry of the cluster test assembly with respect to the PBF driver core, there exists three unique fuel rod types in the nine-rod cluster; the center, side, and corner rods. Two-dimensional transport calculations were performed with RAFFLE⁵, a Monte Carlo code, to determine the fuel rod enrichments which would result in equal power generation within each rod type.

The basic RAFFLE input consisted of a geometric description of the experiment configuration and a description of the energy spectrum for the source neutrons. Since Monte Carlo calculations require large amounts of computer time due to the number of neutron histories which must be followed, the PBF core was not considered in RAFFLE and only the nine-rod cluster was modeled. The neutrons streaming through the cluster from the core are considered as source neutrons whose energy distribution must be specified. SCAMP^a, a one-dimensional

a. SCAMP an unpublished multi-group version of the TOPIC⁶ computer code.

multi-group S_n theory neutron transport code, was used to define the required neutron energy spectrum. A SCAMP calculation was performed, in which the test assembly was represented by annular regions representing the fuel, cladding, and water moderator. The side rods were represented by homogenizing the fuel and associated water, using appropriate thermal disadvantage factors to account for the flux depression across the rod. These rods were then represented as an annulus adjacent to the center rod. The corner rods were similarly homogenized and are represented as an annulus adjacent to the side rods.

The RAFFLE calculations for the test area were performed, using an exact two-dimensional model of the test region. Regions of zircaloy and water were also added 130 mm above and below the fuel, to account for the reflection of neutrons in these regions. Coupling of the test assembly to the PBF driver core was accomplished using the inward directed neutron currents calculated by SCAMP as the external source for the RAFFLE calculations. The axial power distribution used in the calculations was assumed to be cosine shaped, with a peak-to-average ratio of 1.35 over the active fuel region.

Iterative calculations were made to determine the fuel enrichment for each rod type which would result in approximately equal power generation in each of the nine test rods. First, the neutron source spectrum for the RAFFLE calculations was obtained from SCAMP calculations for a 93% enriched center rod and 20% enriched peripheral rods. RAFFLE calculations were then made, varying the enrichments of the side and corner rods until the power level in each rod was about the same. The final enrichments were calculated to be 93%, 35%, and 20% for the center, side, and corner rods, respectively.

The rod powers, as calculated by RAFFLE and SCAMP based on the above fuel enrichments for the nine-rod test assembly, are presented in Table I. The average power for the assembly is 2.07 kW/m per MW of the PBF driver core power and represents approximately 1.7% of the total core power. The average circumferential power distributions

TABLE I

SUMMARY OF CALCULATED ROD POWERS FOR THE 9-ROD TEST ASSEMBLY

| Test Component | Axial Average Power Per Pin ^a (kW/m per MW of Driver Core Power) |
|----------------------------|--|
| 9-Rod Assembly (% of core) | 1.701 (0.007) |
| 9-Rod Assembly (Avg) | 2.068 (0.007) |
| Center Rod | 2.15 (0.021) |
| Side Rod | 2.08 (0.011) |
| Corner Rod | 2.03 (0.011) |

- a. RAFFLE (Monte Carlo) calculations were made, assuming a chopped cosine curve with a 1.35 peak/average ratio over the length of the active fuel. Multiply values in the table by 1.35 to obtain the corresponding peak power densities. Fractional 95% confidence limits, due to statistical uncertainty in the RAFFLE calculations, are shown in parentheses.

510 047

within the fuel rods for one-quarter of the assembly are shown in Figure 2. As shown in the figure, there exists a pronounced power gradient across the side and corner fuel rods. This power skewing, which has not been significant in the previous single rod tests, is caused by the self shielding effects of the peripheral fuel rods. The center rod, which is shielded by the side and corner rods located symmetrically around it, has a relatively flat circumferential power distribution similar to that of previous single rod tests.

2.2 Thermal-Hydraulic Calculations

Since the RAFFLE calculations predicted a circumferentially varying power profile for the peripheral fuel rods, a calculation using TOODEE⁷ was performed to determine the associated azimuthal surface heat flux for each of the fuel rods. TOODEE is a two-dimensional (R,θ) time dependent heat conduction analysis program, which uses the radial and circumferential power profiles as input. The normalized azimuthal surface heat flux, as calculated by TOODEE (using the RAFFLE calculated power profile), are presented in Figure 2. As shown in this figure, the azimuthal surface heat flux factors, calculated for 30 degree segments at various elevations, follow the same basic pattern as that for the circumferential power distribution (also shown in Figure 2). The surface heat flux is greater on the outside of the side and corner rods than on the inside surface. The distribution is relatively flat around the center rod which better represents a fuel rod in a PWR (15x15) array. The determination of the surface heat flux distribution is important because of its direct relationship to the occurrence of stable film boiling operation.

The expected DNB and film boiling behavior for the PCM-5 experiment was calculated using the COBRA-IV¹ computer code. COBRA-IV is a three-dimensional thermal-hydraulic code that solves the equations for conservation of mass, linear momentum, and energy for a number of control volumes that are connected in the radial and axial directions. The fuel rods are modeled explicitly and a temperature

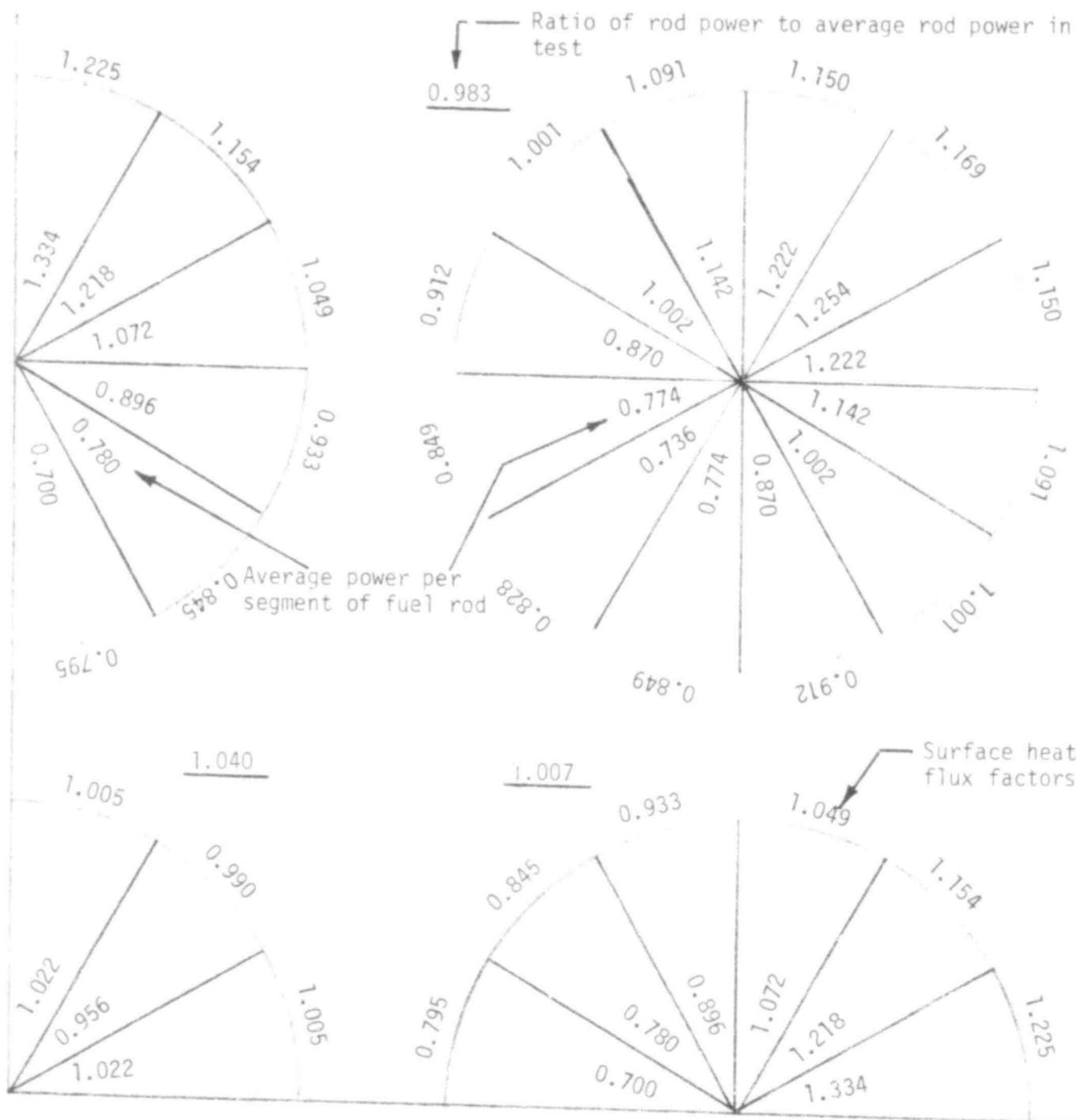


Fig. 2 Average circumferential power and axial surface heat flux factors per 30° segment of fuel rod based on RAFFLE and TOODEE calculations, respectively, for the 9-rod test assembly.

510 049

dependent fuel thermal conductivity is used. The coolant flow area was divided into five subchannels, with boundaries defined by the adjacent fuel rod surfaces, as shown in Figure 3. Empirical and semi-empirical correlations are used to describe such phenomena as turbulent mixing, frictional losses, two-phase flow, and surface heat transfer coefficients. The input parameters, correlations and models used for these COBRA-IV analyses are presented in Appendix A.

2.3 Rod Bowing Calculations

Coolant channel cross-sectional flow area is an important parameter in determining the flow rate at which a fuel rod will enter film boiling. Fuel rod bowing, due to a temperature gradient across the rod, can have a significant effect on the coolant channel flow area. Therefore, knowing how much and in what direction a fuel rod is likely to bow is important.

To estimate the magnitude of rod bowing, the temperature profile (radial, azimuthal and axial) of the fuel rod was specified. FRAP-T4⁹ and TOODEE⁷ calculations were made to determine this temperature profile. Transient FRAP-T4 calculations were made, using the parameters describing a side rod of the PCM-7, nine-rod cluster, at a peak power of 52.5 kW/m and inlet temperature of 590 K. The coolant flow rate was reduced until the rod entered film boiling. The radial and axial temperature profile of the rod just prior to entering film boiling was determined and used in the bowing calculations. Using parameters determined by the physics calculations⁴, TOODEE (R, θ) calculations were conducted. The radial and azimuthal temperature profiles were determined, and used in conjunction with the temperature profiles from the FRAP calculations to develop a three dimensional fuel rod temperature profile.

The calculated three-dimensional fuel rod temperature profile was used as input data to the SAP IV¹⁰ code to make rod bowing calculations of the side rod. The fuel rod was modeled by a solid UO₂ fuel rod column with no radial restraints over the length of the

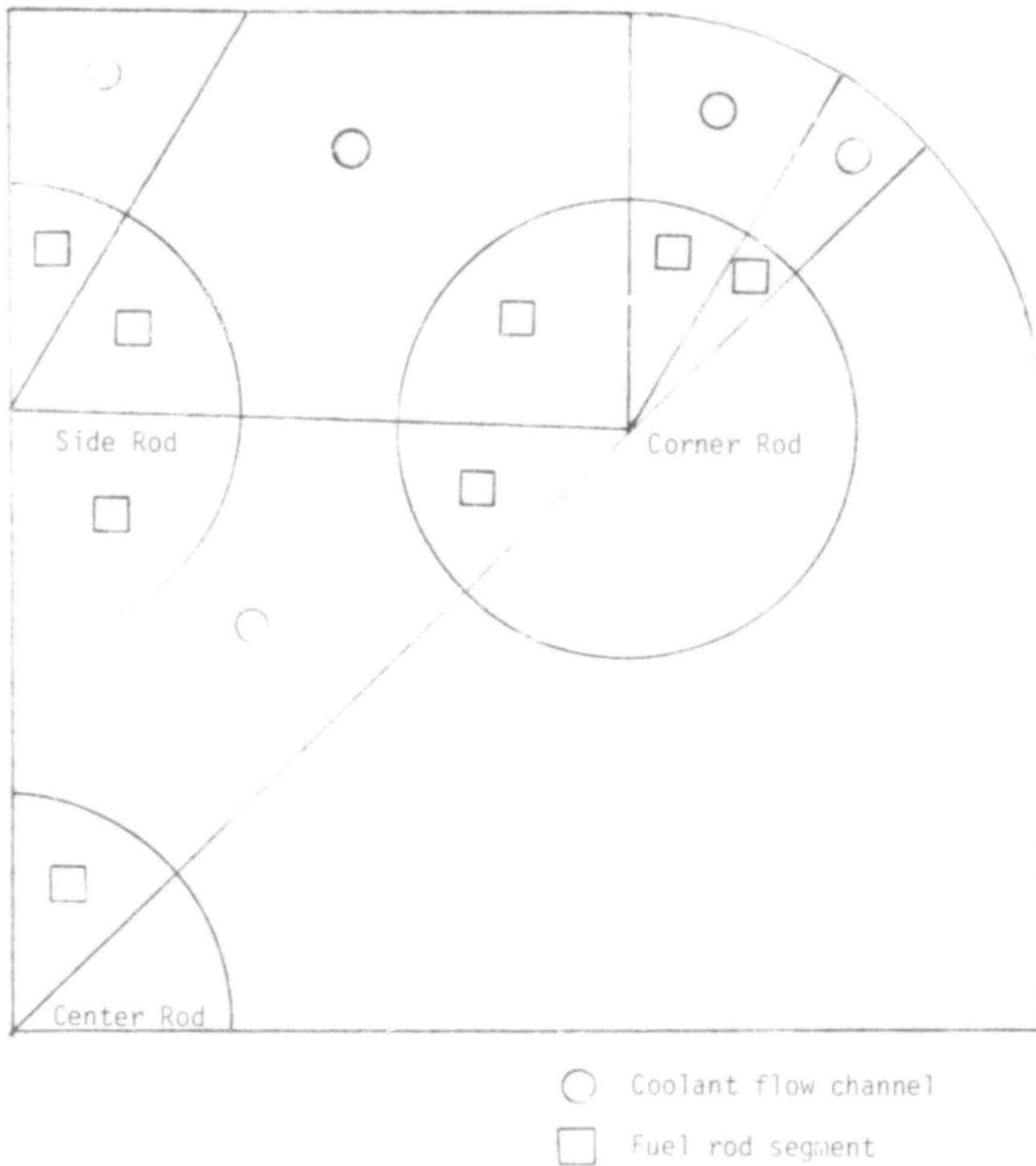


Fig. 3 Model of the 9-rod test assembly showing coolant flow subchannels and corresponding fuel rod segments, used in the COBRA-IV calculations.

fuel stack. The analysis assumed no interaction between the fuel and the cladding (or shroud), and represented a fuel rod in nucleate boiling on the hottest side of the fuel rod at elevations above 0.6 meters. The results of the SAP calculation are shown in Figure 4. Rod bowing above 0.6 meters was inhibited because of nucleate boiling above this elevation.

The bowing calculation performed suggests that bowing of the peripheral fuel rods could have a significant effect on the local subchannel areas and thus, the onset of film boiling. To quantify the effects of rod bowing, an elaborate calculation procedure which includes fuel-cladding interaction and grid spacer effects on rod bowing should be considered. The coupled rod bowing and thermal-hydraulics should then be considered to evaluate the overall cluster behavior. The extensive analysis required to quantify the effects of rod bowing were not performed for test PCM-7.

2.4 Fuel Rod Behavior Scoping Analysis

Calculations were conducted to scope the conditions at the onset of film boiling using the calculated power skewing and measured asymmetry of the cluster from Test PCM-5. The DNB correlation which best predicted the Test PCM-5 observed response was determined using a single subchannel analysis code. COBRA analyses, which includes cross flow between the subchannels, were then conducted using the appropriate DNB correlation to estimate the conditions at incipit film boiling for the various measured subchannel sizes. A schematic of the nine-rod cluster positioned within the flow shroud and the relative dimensions as a result of the measured Test PCM-5 asymmetry is shown in Figure 5. The modeled channel areas for the single subchannel analysis is shown in Figure 6.

The corner rod of Test PCM-5 (205-1) entered film boiling at a coolant mass flux of $1090 \text{ kg/s}\cdot\text{m}^2$, at an averaged peak rod power of 57.1 kW/m and an inlet temperature of 590 K . Using the PCM-5 conditions and the calculated flow area for Rod 1, the subchannel

510 052

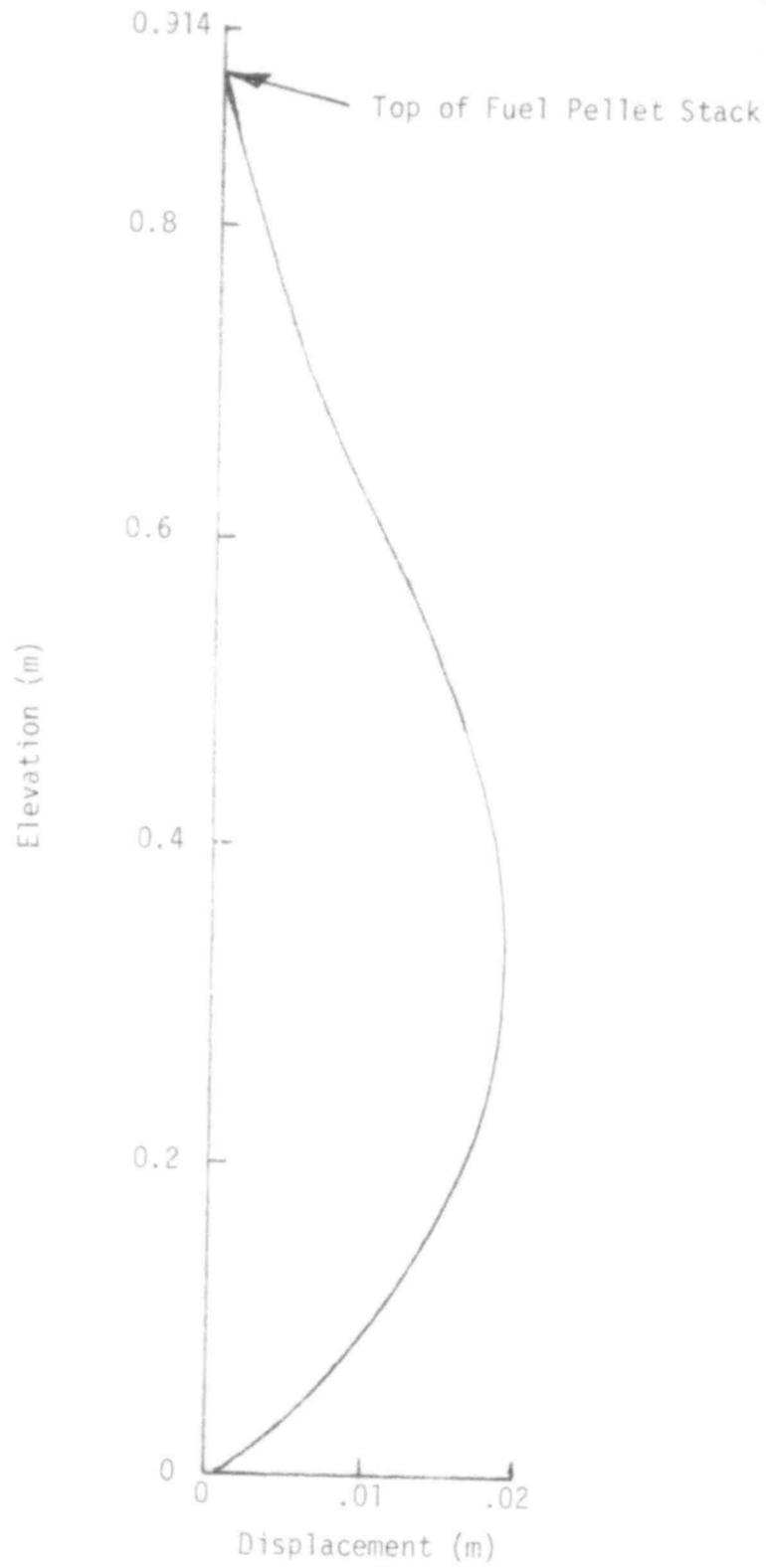


Fig. 4 Calculated fuel rod displacement due to bowing caused by temperature gradient across the rod from neutron self shielding.

510 053

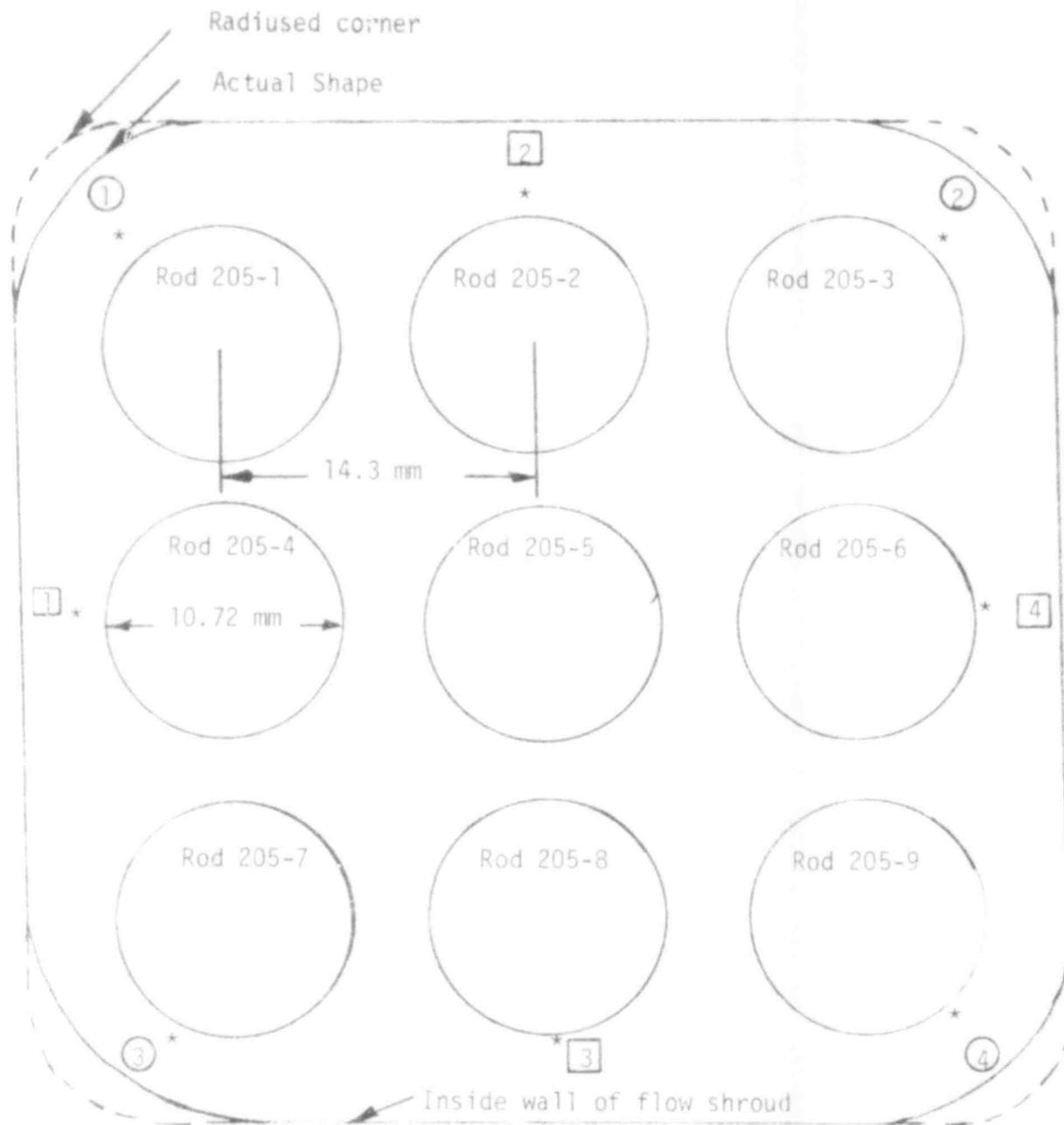


Fig. 5 Test PCM-5 assembly showing fuel rod diameters, lattice spacing and shape of flow shroud.

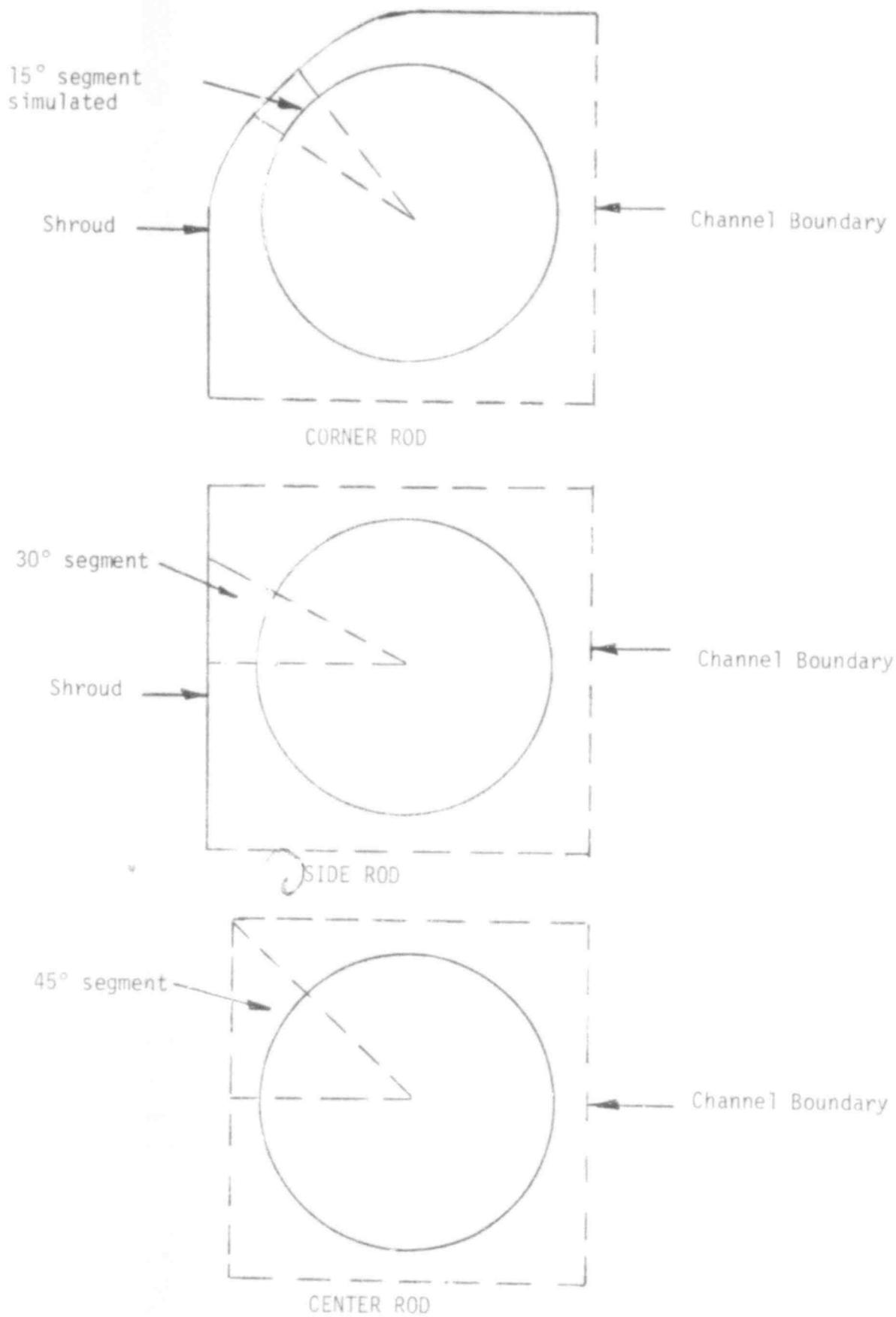


Fig. 6 Geometry used to simulate single channel analysis of corner, side and center rods.

510 055

analysis best predicted the actual flow rate at which film boiling was attained when using the B&W-2 critical heat flux (CHF) correlation. The B&W-2 CHF correlation predicted film boiling would first occur at a coolant mass flux of approximately $1250 \text{ kg/s}\cdot\text{m}^2$. Both the W-3 and LOFT correlations were considered, but predicted film boiling to occur at a coolant mass flux $>1700 \text{ kg/s}\cdot\text{m}^2$.

Scoping calculations (COBRA) were performed for Test PCM-7 using the minimum, maximum, and average subchannel areas determined from the Test PCM-5 pretest characterization. The heat flux produced in each modeled segment (Figure 3) was determined from the physics and COBRA calculations, and then performed for the three subchannel size cases. In each case, the coolant mass flux was reduced at constant power (57.1 kW/m) and inlet temperature (605 K) until film boiling was indicated on all rod types. The results of the three calculations are presented in Table II.

The COBRA calculations indicate that film boiling could be achieved at a flow rate as high as $1880 \text{ kg/s}\cdot\text{m}^2$ (minimum channel area) on the corner rod and as low as $1265 \text{ kg/s}\cdot\text{m}^2$ on the center rod. The calculations indicate that the corner and side rods of the 9-rod bundle could enter film boiling in any sequence, depending upon the flow area between the rods and the flow shroud. Mixing between the coolant channels of the side and corner rods (see Figure 3) was calculated to be less than 6%, however, the mixing between the center rod coolant channel and the peripheral rod channels was calculated to be as high as 36% near the grid spacers. The mixing of the coolant from the coolest side of the peripheral fuel rods with the coolant around the center rod causes the center rod to attain film boiling conditions at a lower coolant flow rate than the peripheral rods.

The COBRA calculations for the average channel flow areas were continued until stable cladding temperatures (approximately 30 seconds) were achieved on all rods. The peak cladding surface temperatures at 10 and 20 seconds after film boiling first occurred are shown for the modeled rod segments in Figure 7. The calculated

510 056

TABLE II

FILM BOILING FLOW RATES CALCULATED BY COBRA^a

| Rod Type | Coolant Flow Rate at Which Rod Achieved Film Boiling | | |
|----------|--|---|---|
| | Minimum Channel Flow Areas (kg/s·m ²) | Average Channel Flow Areas (kg/s·m ²) | Maximum Channel Flow Areas (kg/s·m ²) |
| Corner | 1880 | 1790 | 1455 |
| Side | 1565 | 1495 | 1385 |
| Center | 1265 | 1265 | 1265 |

^a All calculations at 57.1 kW/m peak rod power (average per rod), 605 K inlet temperature, and using the B&W-2 CHF correlation.

510 057

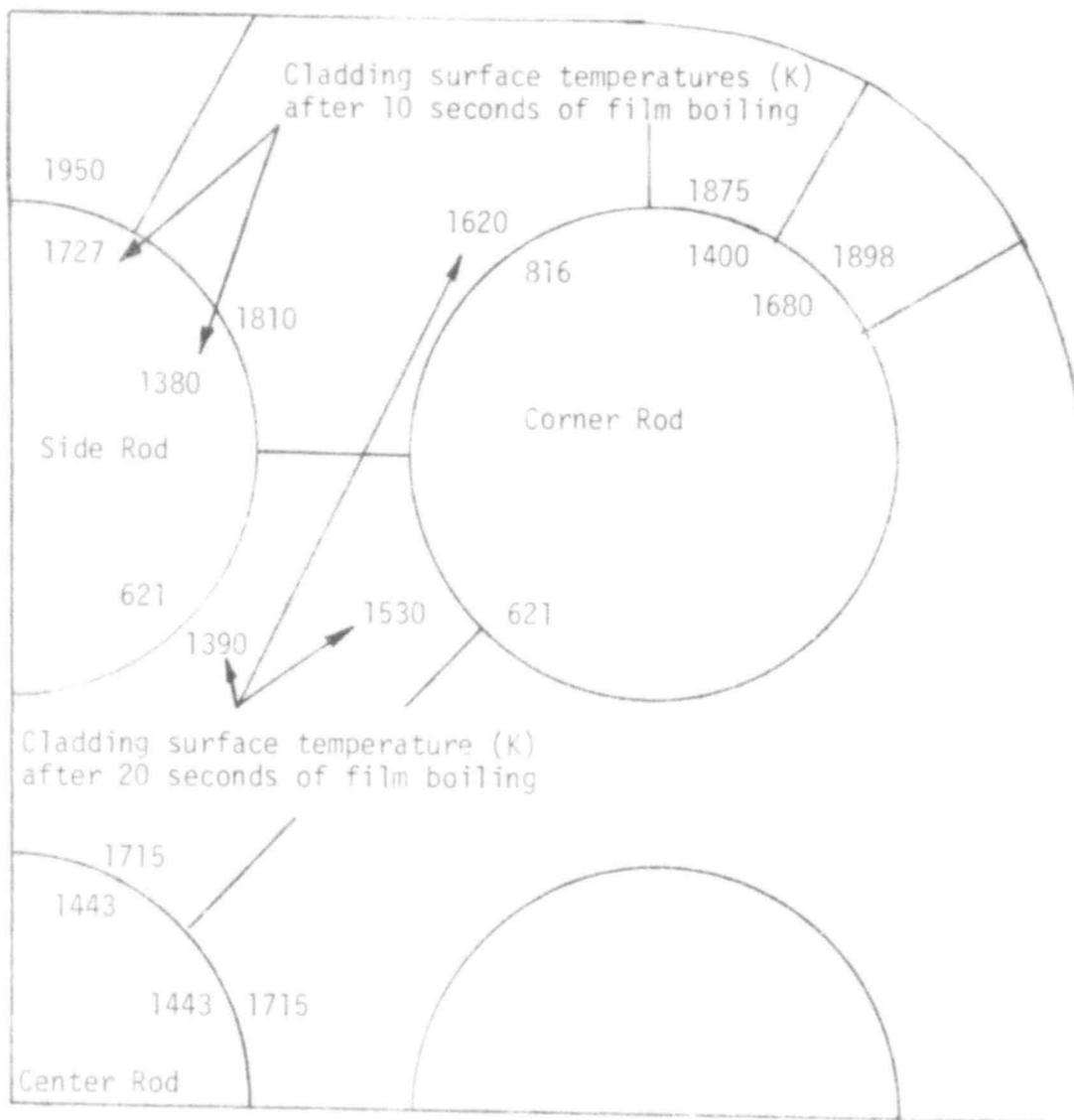


Fig. 7 PCM-7 rod cluster peak cladding temperatures after approximately 10 and 20 seconds of film boiling and an inlet coolant temperature of 605 K and a power of 57.1 kW/m. All values inside of rod sketch perimeter are 10 s values - outside are 20 s values.

azimuthal power skewing resulted in large predicted temperature gradients on the peripheral rods. The peak cladding surface temperature as a function of time for a corner rod, side rod, and the center rod are presented in Figure 8. COBRA predicts the side rod will experience the highest cladding surface temperature after film boiling is well established. The maximum temperatures predicted (about 28 seconds after film boiling first occurs) are 1990 K for the side rod, 1900 K for the corner rod, and 1770 K for the center rod.

510 059

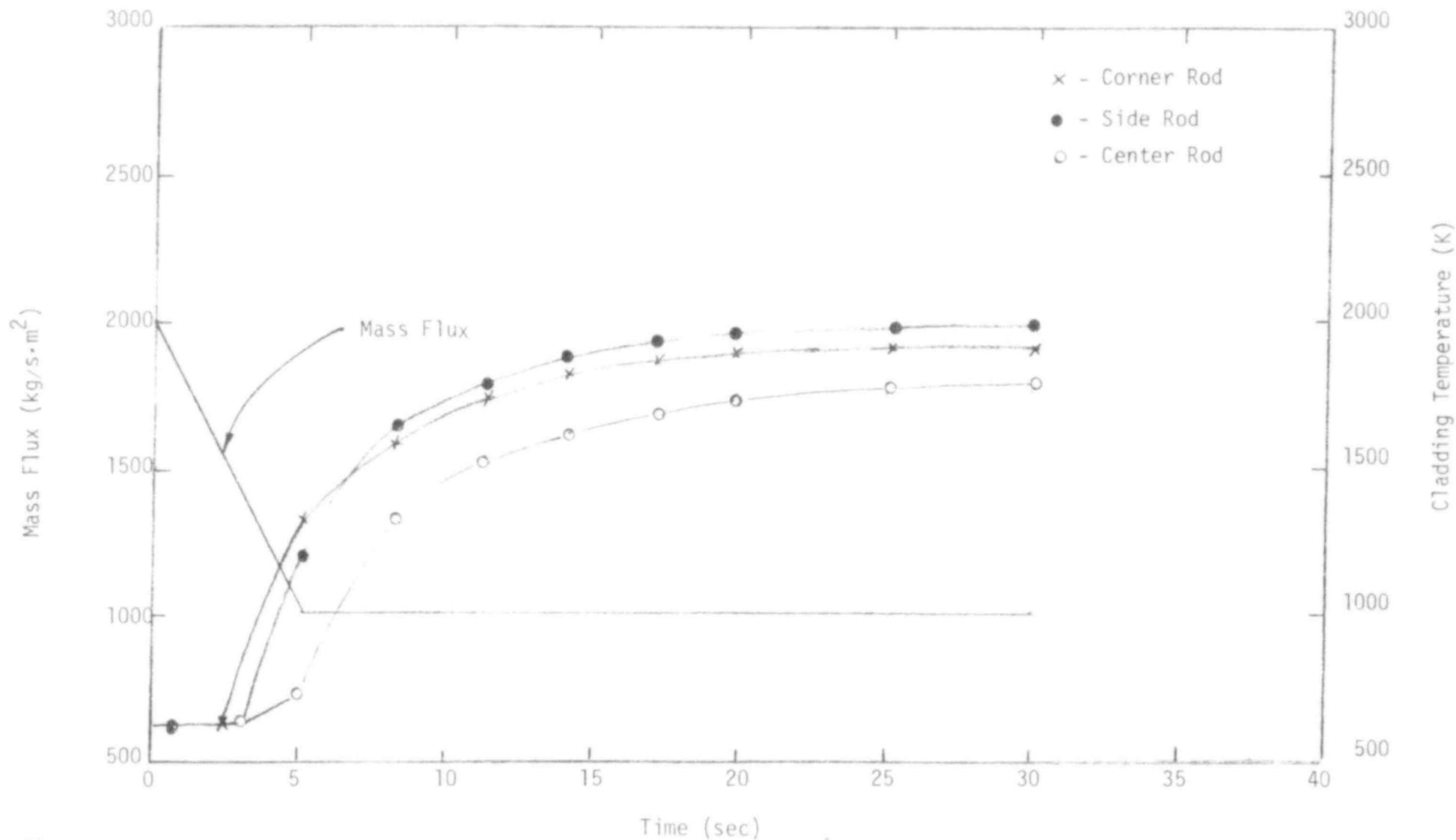


Fig. 8 Peak cladding surface temperature as a function of time for corner, side, and center rods of a PCM nine-rod cluster. Inlet temperature 605 K, averaged peak rod power 57.1 kW/m.

510 060

3. EXPERIMENT PREDICTIONS

The final portion of Test PCM-7 will include extended film boiling operation within the cluster. The test rod power will be increased to induce film boiling within the assembly, but is not expected to result in film boiling on all test rods. The shroud flow rate will subsequently be reduced until film boiling on the center rod is achieved, and operation continued until rod failure is detected. Rewet of all rods will then be attempted by increasing the flow rate at constant power conditions. This section describes the computer code "best estimate" predictions of the onset of film boiling and the behavior of each rod type to film boiling conditions.

3.1 On-Set of Film Boiling

COBRA calculations were performed to predict the coolant conditions at the onset of film boiling for each rod type (corner, side and center). For these calculations, the cluster was assumed to be symmetrically positioned within the shroud, and the resulting subchannel dimensions the same as the averaged dimensions determined from Test PCM-5. The calculated azimuthal power skewing was considered in the same manner as the previously described scoping calculations. All calculations were conducted with a rod power (weighted average per rod at the peak power location) of 57.1 kW/m and coolant inlet temperature of 605 K. The input parameters, correlation description, and models used for the COBRA IV analysis are presented in Appendix A.

The onset of film boiling was predicted to occur initially on the outside (high heat flux) segment of the corner rods at a mass flux of $1790 \text{ kg/s}\cdot\text{m}^2$ at an elevation 0.71 m above the bottom of the fuel stack. Further reduction of the shroud flowrate resulted in film boiling conditions on the side rods at $1495 \text{ kg/s}\cdot\text{m}^2$ mass flux, and on the center rod of $1265 \text{ kg/s}\cdot\text{m}^2$ mass flux.

510 061

3.2 Fuel Rod Behavior

The FRAP-T4⁹ computer code was used to calculate the behavior of the PCM-7 fuel rods using the predicted coolant conditions from the COBRA analysis. With these conditions, the calculated fuel rod behavior to the predicted thermal-hydraulic environment was obtained. A description of the FRAP-T4 model used for the PCM-7 analysis is presented in Appendix B.

The corner rod cladding and fuel centerline temperatures were calculated at various flow rates below the flow required to induce film boiling on the rods. The peak calculated temperatures on the corner rods are shown for 3 and 35% flow reductions in Figure 9. The 3% reduction ($1736 \text{ kg/s}\cdot\text{m}^2$ coolant mass flux) represents the level at which the extended film boiling operation will be initiated. The 35% reduction level ($1164 \text{ kg/s}\cdot\text{m}^2$ coolant mass flux) represents the predicted level at which the center rod cladding temperatures will exceed 1245 K (the β -zircaloy temperature regime). At the lower flowrate, a small axial extent ($<16 \text{ mm}$) of centerline fuel melting is predicted. Cladding melting ($T > 2100 \text{ K}$) is not predicted at any elevation. The corner rod peak cladding temperature as a function of flowrate is shown in Figure 10, where 100% represents the flowrate at the point of film boiling initiation.

The proposed test conduct outlined in the PCM-7 EOS³ was used in conjunction with Figure 11 to estimate the time to rod failure during high temperature operation¹². The estimated time to corner rod failure and the remaining β -zircaloy (fraction) remaining at each of the flow reductions identified are listed in Table III. The composite oxide and oxygen stabilized α -Zr layer thicknesses for the proposed operating sequence, resulted in a calculated "at power" rod failure time of approximately 28 minutes after film boiling initiation. The failure time estimate corresponds to film boiling operation on the center rod for approximately 8 minutes.

510 062

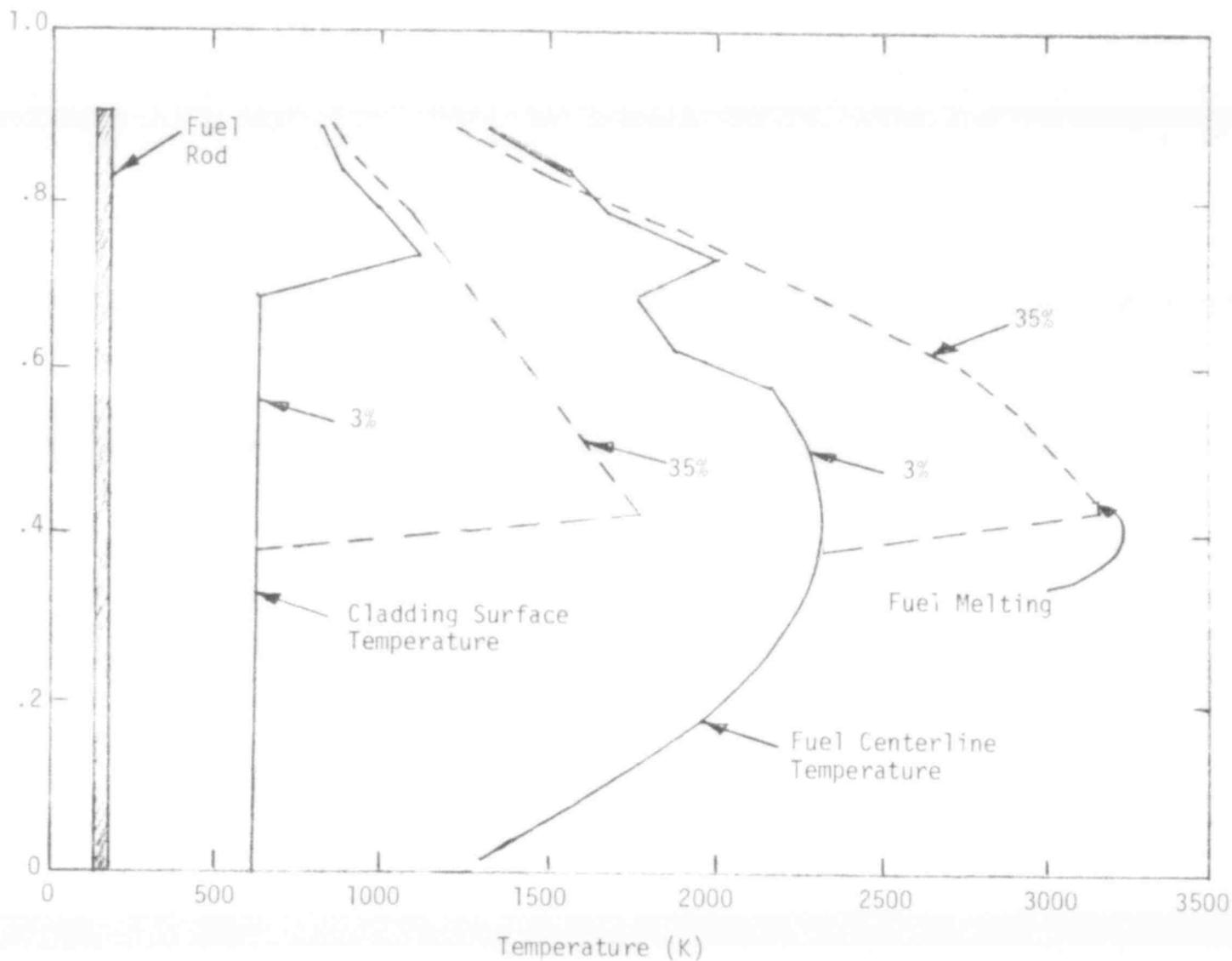


Fig. 9 Axial temperature profile for the cladding surface and fuel centerline calculated by FRAP-T for an average corner rod at a peak power of 57.1 kW/m, coolant inlet temperature of 605 K, and mass flux of 1736 and 1163 kg/s·m² (3% and 35% below calculated initiation of film boiling).

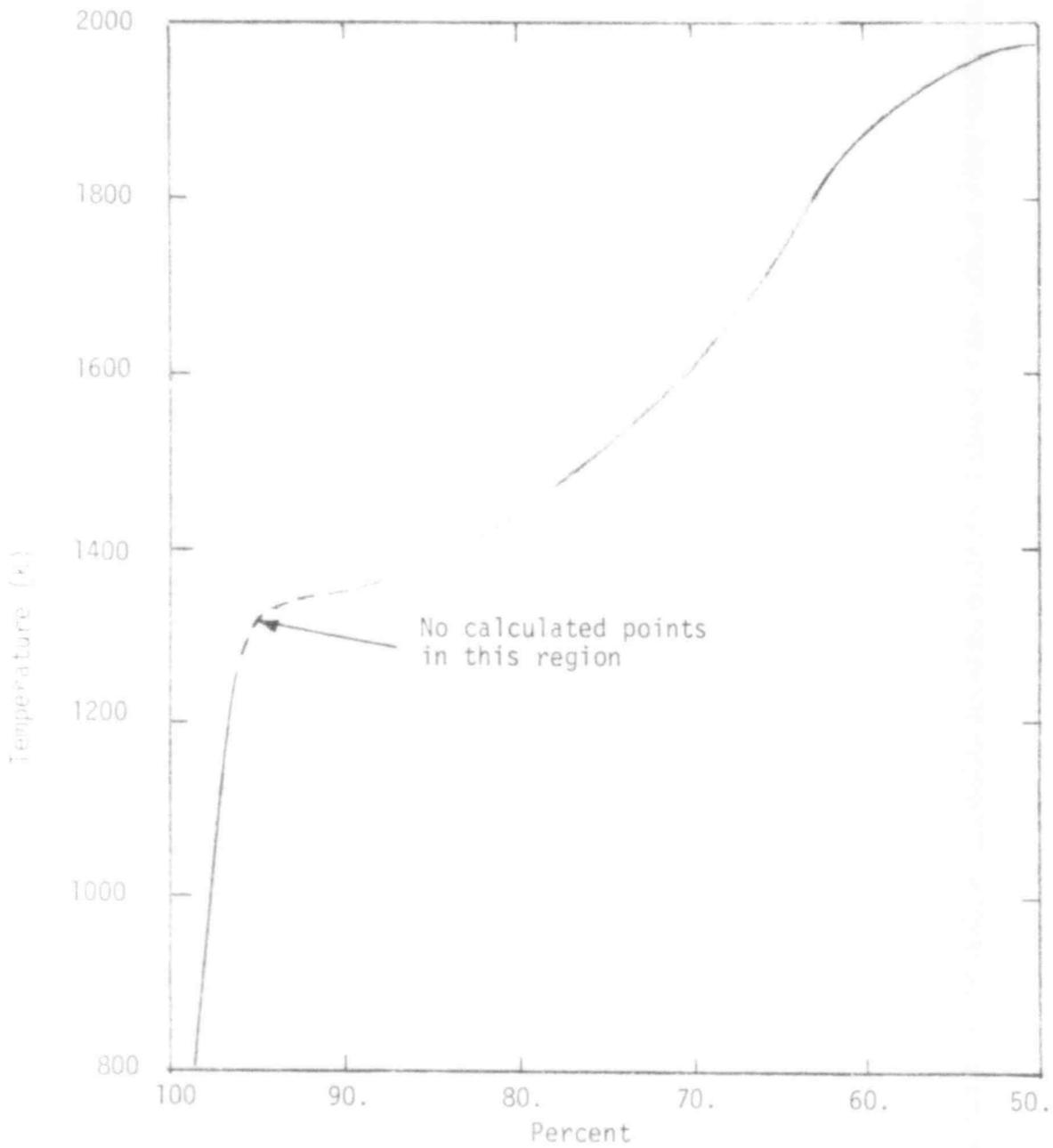
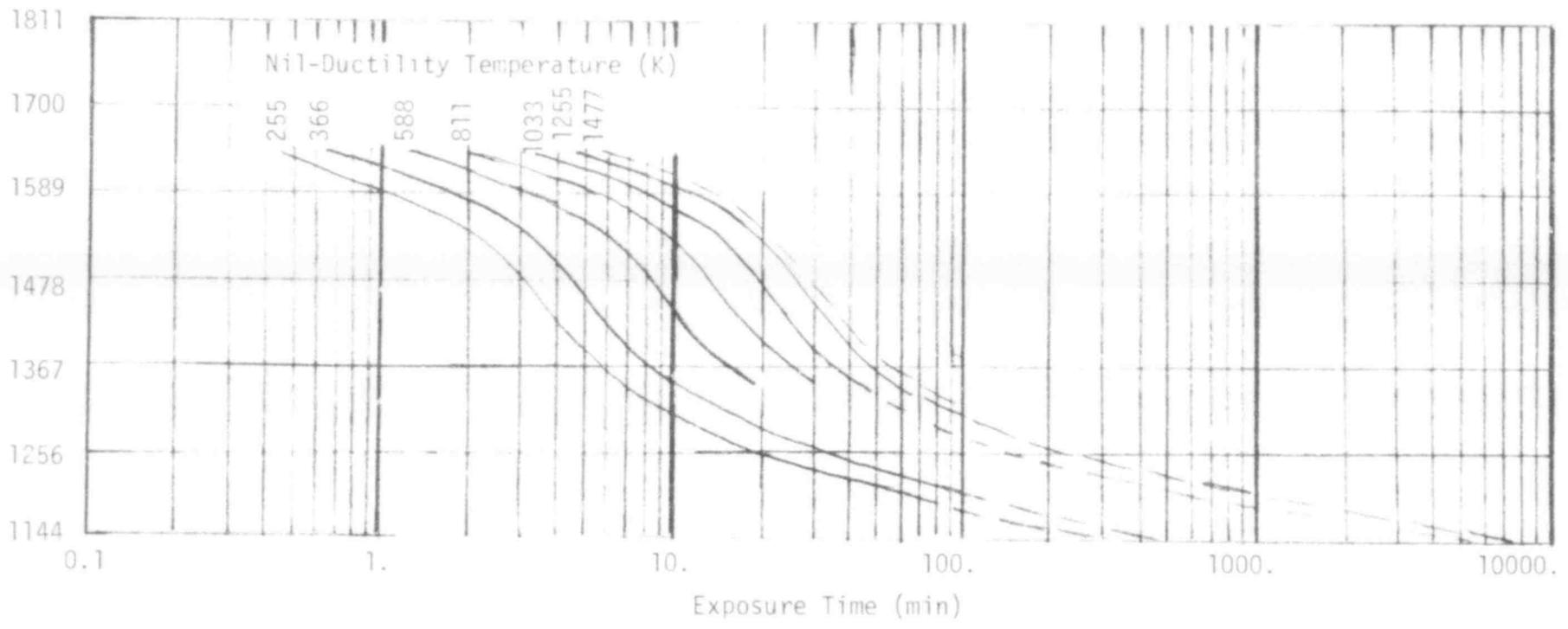


Fig. 10 Peak cladding surface temperature as a function of coolant mass flux percent where 100% represents the point of initial film boiling, PCM-7 corner rod.

27



510 065

Fig. 11 Nil-Ductility temperature as a function of exposure time and temperature from Reference 12. Dashed lines are extrapolations.

TABLE III

FUEL ROD RESPONSE AS A FUNCTION OF COOLANT MASS FLUX REDUCTION
FOR THE CORNER RODS OF TEST PCM-7

| Percent Mass Flux ^a | Peak Cladding Surface Temp. (K) | Peak Temperature Elevation (m) | Time to Isothermal Rod Failure ^b | Fraction of Cladding Wall Which is β Phase Zinc at Isothermal Failure Time | Corner Rod Peak Fuel Temp. (K) | Extent of Film Boiling (m) | | | Variation due to Measured Assymetry ^c |
|--------------------------------------|--|---|--|---|--------------------------------------|----------------------------|-------------|---------------|---|
| | | | | | | Corner Rod | Side Rod | Center Rod | |
| 97 | 1100 | 0.68 | 150 hrs | Not Calculated | 2319 | 0.65-0.78 | -- | -- | Corner +8%-16% |
| 90 | 1345 | 0.63 | 70 min | 0.71 | 2440 | 0.55-0.86 | -- | -- | |
| 85 | 1380 | 0.58 | 55 min | 0.69 | 2780 | 0.52-0.91 | 0.63-0.68 | -- | Side +5%-7% |
| 80 | 1445 | 0.53 | 40 min | 0.62 | 3030 | 0.50-0.91 | 0.57-0.73 | -- | |
| 75 | 1520 | 0.51 | 30 min | 0.52 | 3085 | 0.47-0.91 | 0.52-0.78 | -- | |
| 70 | 1610 | 0.48 | 15 min | 0.49 | 3110 | 0.44-0.91 | 0.50-0.78 | 0.63-0.78 | Center |
| 65 | 1640 | 0.43 | 6 min | 0.48 | 3141 | 0.44-0.91 | 0.47-0.78 | 0.55-0.78 | |

a. 100% mass flux represents the point of initiation of film boiling which will occur on a corner rod.

b. Estimated using Figure 11.

c. Coolant mass flux rate at which fuel rods are most likely to enter film boiling and variation determined from PCM-5 nominal channel flow area measurements.

510

066

Table III also presents the corner rod peak fuel centerline temperature and the axial extent of film boiling on each rod type at the flow reduction levels considered. The axial extent of film boiling was determined from the COBRA analysis for a symmetrically positioned cluster, since the FRAP-T analysis did not consider the affect of grid spacers on film boiling operation. The calculated variation in coolant mass flux at DNB initiation due to the observed cluster asymmetry (from Test PCM-5) is also listed in Table :

The axial flux centerline and cladding surface temperature profiles for the side and center rods are shown at the 35% flow reduction level in Figures 12 and 13. The peak temperatures on the side rods are predicted to occur at the 0.55 m elevation. Cladding temperatures of approximately 1450 K and a centerline temperature of 2800 K are predicted for the side rods (for a symmetrically positioned cluster). A peak cladding temperature of 1240 K is predicted for the center rod at the 35% flow reduction level.

The phenomena of rewet is not well understood and hence is not adequately modeled by state-of-the-art computer codes. The return to nucleate boiling (from film boiling operation) conditions for Test PCM-7 were not predicted since meaningful results could not be expected.

510 067

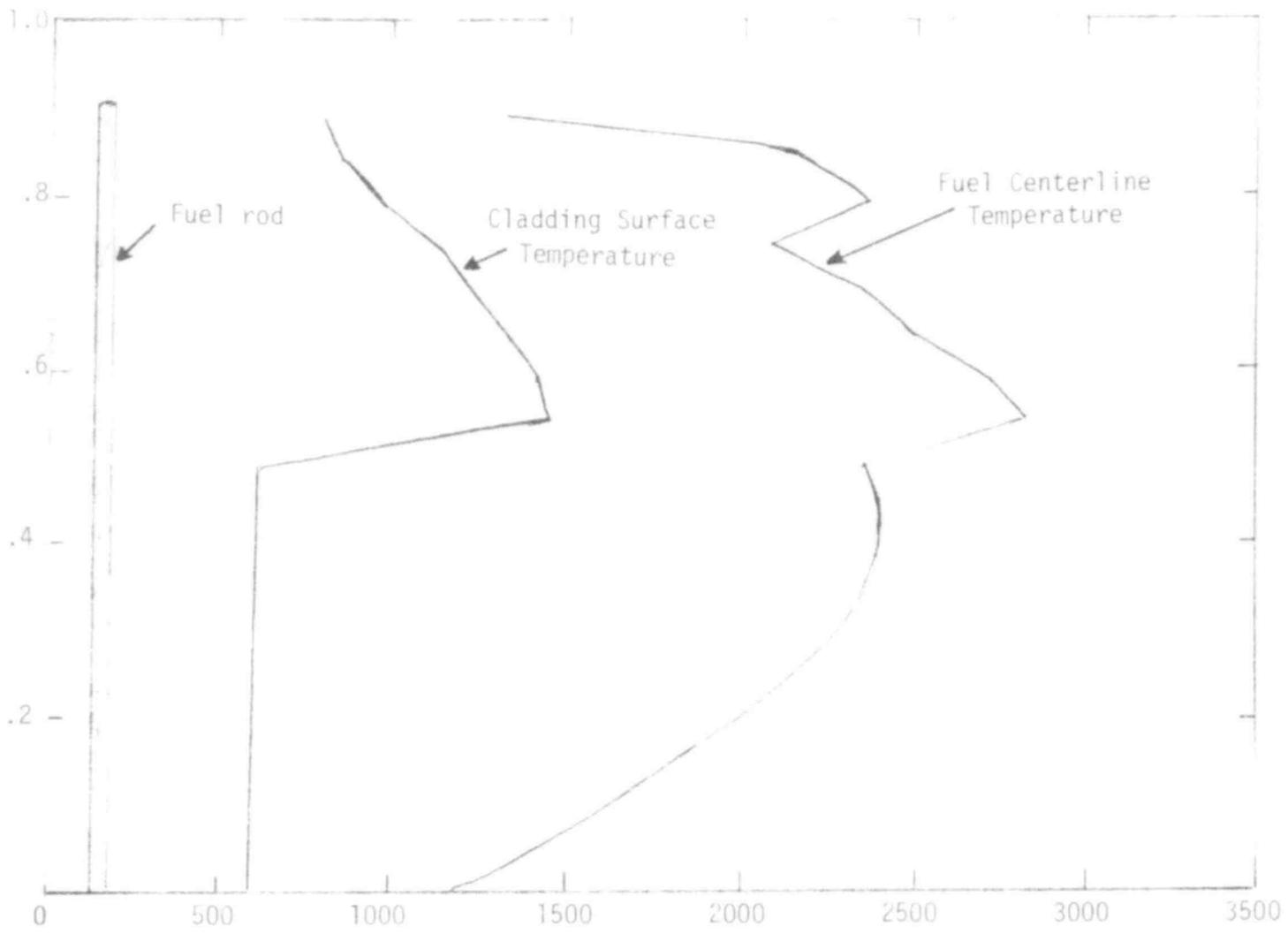


Fig. 12 FRAP-T calculated temperature profile for the cladding surface and fuel centerline of a side rod at the 35% flow reduction level ($1163 \text{ kg/s}\cdot\text{m}^2$). Test rod power of 57.1 kW/m and inlet temperature of 605 K .

30

510
063

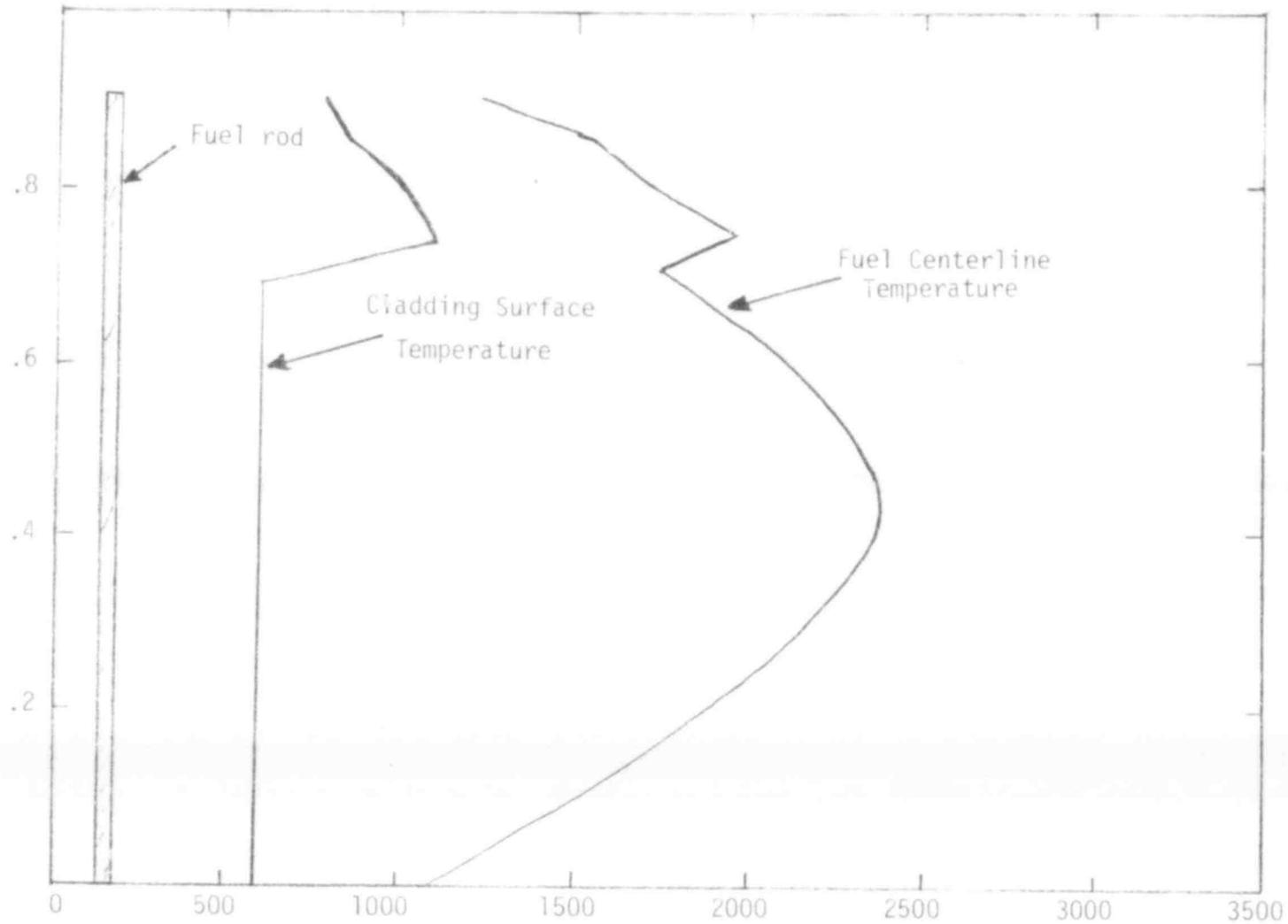


Fig. 13 FRAP-T calculated temperature profile for the cladding surface and fuel centerline of the center rod at the 35% flow reduction level ($1163 \text{ kg/s}\cdot\text{m}^2$). Test rod power of 57.1 kW/m and inlet temperature of 605 K .

510 069

4. DISCUSSION

Based on the analysis performed for Test PCM-7, film boiling will occur initially on the corner rods of the bundle, and with further flow reductions, will occur on the side and center fuel rods. Results from Test PCM-5 suggest that direct rod-to-rod interactions should not be expected, but several factors may effect the onset of film boiling in the assembly. The factors which may effect the film boiling behavior of the PCM-7 cluster but were not explicitly determined include; peripheral rod bowing, cluster asymmetry, thermocouple effects, and two-phase coolant instabilities. Thermocouple effects and two-phase instabilities may be especially important in determining the rewet characteristics of the cluster.

The COBRA-IV and FRAP-T4 calculations indicate that stabilized cladding temperatures in the high temperature β -phase region ($T = 1245$ K) will be evident at incipit film boiling on the central rod. Center rod cladding temperatures near the β -phase region are expected. Peripheral rod failure due to cladding embrittlement is anticipated following several minutes of high temperature film boiling operation. Cladding melting is not expected and the small amount of local fuel melting is not expected to cause early rod failure.

The Test PCM-7 conduct was designed to allow verification of the Test PCM-5 results, and help evaluate the important parameters during rewet from film boiling operation. The return to nucleate boiling from high temperature is a complex phenomena, which in general, is not predicted by current computer codes. An understanding of the rewet process is, therefore, of fundamental interest in reactor safety analysis.

510 070

5. REFERENCES

1. C. L. Wheeler et al, COPRA-IV: An Interim Version of COBRA for Thermal-Hydraulic Analysis of Rod Bundle Nuclear Fuel Elements and Cores, BNWL-1962, UC-32 (March 1976).
2. J. M. Broughton, Light-Water Reactor Fuel Behavior Program Description: PCM Fuel Behavior Experiment Requirements, SRD-106-76 (May 1976).
3. D. T. Sparks, R. H. Smith, and C. J. Stanley Power-Cooling-Mismatch Test Series Test PCM-7, Experiment Operating Specification, TFBP-TR-191 (May 1977).
4. T. E. Young, Physics Calculations for the PCM-5 Test, RE-P-77-081 (October 1977).
5. W. E. Weseley, F. J. Wheeler, and R. S. Marsden, The RAFFLE General Purpose Monte Carlo Code, ANCR-1022 (April 1973).
6. G. E. Putnam, TOPIC - A Fortran Program for Calculating Transport of Particles in Cylinders, IDO-16968 (April 1964).
7. J. A. McClure, TOODEE: A Two Dimensional, Time-Dependent Heat Conduction Program, IDO-17227 (April 1967).
8. C. J. Stanley and W. F. Domenico, Power Coolant Mismatch Test Series Test PCM-5 Experiment Predictions, TFBP-TR-239 (December 1977).
9. J. A. Dearian, L. J. Seifken, and M. P. Bohn, FRAP-T4, A Computer Code for the Transient Analysis of Oxide Fuel Rods, CDAP-TR-78-027 (July 1978).
10. K. J. Bathe, E. L. Wilson, and F. E. Peterson, "SAP IV, A Structural Analysis Program for Static and Dynamic Response of Linear Systems", Earthquake Engineering Research Center, University of California, Berkeley, (June 1973).
11. P. E. MacDonald and W. F. Domenico, PCM-9 Rod Cluster Position Paper, TFBP-TR-224 (October 1977).
12. D. O. Hobson and P. L. Ritterhouse, Embrittlement of Zircaloy-Clad Fuel Rods by Steam During LOCA Transients, ORNL 4758 (January 1972).

510 071

APPENDIX A

COBRA-IV INPUT PARAMETERS, CORRELATIONS, AND
MODELING OPTIONS

510 072

APPENDIX A

COBRA-IV INPUT PARAMETERS, CORRELATIONS, AND MODELING OPTIONS

Subchannel analyses were performed for the PCM-7 test assembly coolant conditions, using the COBRA-IV computer code. The code computes coolant flow and enthalpy distributions in the fuel rod bundle for both steady-state and transient conditions. Table A-I presents a list of the input parameters, correlations and modeling options which were used in the final COBRA-IV analysis of the assembly.

510 073

TABLE A-I

INPUT PARAMETERS, CORRELATIONS AND MODELING OPTIONS USED IN
THE COBRA-IV CALCULATIONS

Friction Factor Correlation:

$$\text{FRICTION} = 0.023 \text{ Re}^{-0.2}$$

Wall viscosity correction not included

Single Phase Heat Transfer Correlation:

$$\text{HFILM} = \frac{K}{D_H (0.023 \text{ Re}^{0.8} \text{ Pr}^{0.4})}$$

Two Phase Flow Correlations:

No subcooled void correlation

Homogeneous bulk void model

Homogeneous model friction multiplier

Heat Flux Distribution

Subchannel Input Data

Rod Input Data

Thermal Properties of Fuel Material and Clad Material

Non-uniform Fuel Thermal Conductivity:

$$\frac{K}{K_0} = 1 - 0.59475 \text{ E-3 } (T-T_0) + 0.18030 \text{ E-6 } (T-T_0)^2 - 0.16130 \text{ E-10 } (T-T_0)^3$$

Explicit Solution with inlet flow specified

Start run from an implicit solution

Calculation Parameters:

Lateral resistance factor = 0.5

S/L Parameter = 0.25

Turbulent momentum factor = 0.0

Vertical fuel rods and channels

Channel length = 0.9335 m (36.75 in)

Number of axial nodes = 35

510 074

TABLE A-I(continued)

Implicit solution data

Explicit solution data

Mixing Correlations:

Subcooled mixing, $BETA = 0.062 \left(\frac{D}{S}\right) Re^{(-0.1)}$

Boiling mixing, BETA assumed same as for subcooled mixing

Operating conditions:

Fuel Rod Power = 57.13 kW/m

System Pressure = 15.25 MPa

Inlet Enthalpy = 1.534 MJ/kg

Average mass velocity = 1000 kg/s·m²

Inlet temperature = 605 K

Average Power = 57.13 kW/m

Uniform inlet enthalpy

Uniform inlet mass velocity

Forcing functions for heat flux

Forcing functions for inlet flow

510 075

APPENDIX B

FRAP-T4 INPUT PARAMETERS, CORRELATIONS
AND MODELING OPTIONS

510 076

APPENDIX B

FRAP-T4 INPUT PARAMETERS, CORRELATIONS AND MODELING OPTIONS

The fuel rod characteristics associated with the coolant conditions predicted by COBRA-IV calculations were analyzed using the FRAP-T4 computer code. The FRAP-T4 code is a transient fuel rod thermal analysis code used to solve for the response of fuel rods under various accident conditions. Table B-I presents a listing of the input parameters, correlations and modeling options used in the final FRAP-T4 fuel analysis of the Test PCM-7 center rod.

510 577

TABLE B-I

INPUT PARAMETERS, CORRELATIONS AND MODELING OPTIONS USED IN
THE FRAP-T4^a CALCULATIONS

Number of Fuel Rods = 1
Number of Flow Channels = 1
Number of Axial Nodes = 18
Number of Radial Nodes = 11
Fuel Deformation Model Type = 0
Free Thermal Expansion Fuel Deformation Model Specified
Cathcart Cladding Oxidation Model Specified
Modified Ross and Stoute Model for Gap Conductance Used
Gas Flow Model Turned On
Critical Heat Flux to be Multiplied by a Factor of 1.0
Fuel Rod Length = 0.914 m
Rod Diameter = 0.0107 m
Cladding Cold Work = 0.1
Probability Threshold for Fuel Rod Failure = 1.1
Fuel Pellet Dimensions and Composition Data
Normalized Axial Variation in Fast Flux Assumed Same as that of Fuel Rod Power
Thermal Property Data for Clad and Fuel
Geometry and Composition Specifications
Radial Power Distribution
Initial Temperature Distribution = 605 K
Central Void Prescribed and Modeled for Fuel
Average Power for Fuel Rod
Axial Power Profile
Core Pressure = 15.17 MPa
Heat Transfer Coefficients
Bulk Temperature
Arithmetic Mean Roughness of Cladding and Fuel Specified:
 Cladding = 1.14 μm
 Fuel = 2.12 μm
B&W-2 CHF Correlation
Initial Gas Fill Information:
 Composition = helium (100%)
 Pressure = 2.585 MPa
 Temperature = 300 K

a. FRAP-T, MOD004, VER 06/23, MATPRO MODULE MOD010

510 078